ELSEVIER

Polymer Vol. 37 No. 15, pp. 3273–3281, 1996

0032-3861/96/$15.00+0.00

Tensile drawing of poly(aryl ether ether ketone): 2. Analysis of the stress–strain–orientation relationships through the Brown and Windle model

Véronique Bassigny and Roland Séguéla*
Laboratoire de Structure et Propriétés de l'Etat Solide, URA CNRS 234, Université de Lille I, 59655 Villeneuve d'Ascq Cedex, France

and François Rietsch
Laboratoire de Caractérisation des Matériaux Polymères et Composites, Ecole Universitaire d'Ingénieurs de Lille, Université de Lille I, 59655 Villeneuve d'Ascq Cedex, France
(Received 15 August 1994; revised 11 July 1995)

The deformation behaviour of amorphous poly(aryl ether ether ketone) films above the glass transition temperature is studied by analysing the amorphous orientation function and shrinkage stress variations *versus* draw ratio in the framework of the two component model of Brown and Windle which considers separate orientational and extensional contributions to the overall strain. This analysis is in line with our previous conclusion of the existence of two regimes dominated by orientation of rigid structural units and extension of the chains before and after the threshold of the strain-induced crystallization, respectively. Also supported is the disentanglement trend of the chains prior to the crystallization which brings about a physical crosslinking effect to the macromolecular network. The identification of the rigid structural unit with a single monomer unit is remarkably consistent with our previous determination of the size of the random link. The study of isothermally-crystallized samples supports the conclusion about the efficiency of the crystallites for preventing chain slippage. The estimation of the molecular weight between entanglements as a function of draw ratio for both amorphous and crystallized samples suggests that the physical crosslinking effect of the crystallites is much more efficient than the intertwining of the chains. Copyright © 1996 Elsevier Science Ltd.

(Keywords: poly(aryl ether ether ketone); orientation; shrinkage stress)

INTRODUCTION

The study of the orientational behaviour of semi-crystalline polymers upon drawing is a step of prime importance in the knowledge of the mechanical properties from which the processing conditions can be set up to impart well-determined use properties. A number of methods have been developed to assess separately the crystalline and the amorphous chain orientations[1,2]. Comparison of data from several techniques is often required for better confidence.

Modelling the deformation behaviour is particularly helpful for understanding the mechanism of chain unfolding and orientation and the accompanying improvement of the mechanical properties of drawn polymers. Two main models have been developed to describe the deformation of polymer networks in the rubbery state. On the one hand, the affine deformation scheme based on the statistical mechanics of non-gaussian chain molecules[3,4] is likely to account for the strain-hardening effect due to the limited extension of the network in crosslinked rubbers as well as semi-crystalline flexible chain polymers. Some refinements have been brought about in order to provide better fit of the predicted orientation–strain[4,5] and stress–strain[6,7] variations with the experimental data. On the other hand, the pseudo-affine deformation scheme based on the aggregate model[8] assumes that the polymer consists of rigid units embedded in a continuum, each of the units being able to rotate without change of length. This latter scheme dealing only with the orientation–strain behaviour is generally more appropriate for semi-crystalline polymers which usually develop strong orientation at low strains.

Poly(aryl ether ether ketone) (PEEK) has received increasing attention in recent years because of its high performance properties and its capability for processing as a thermoplastic composite matrix. Some investigations dealing with the molecular orientation of drawn PEEK have been reported. Birefringence *versus* draw ratio measurements from various sources exhibit some discrepancies about the fine features of the variation and the maximum attainable birefringence[9–11]. Serious disagreement has appeared as concerns the determination of crystal orientation from X-ray diffraction data[12–14] because of the amorphous scattering that overlaps the

* To whom correspondence should be addressed

crystalline reflections. Infrared dichroism measurements have been also a matter of controversy[11,15–19] because of the uncertainty in the assignment of some of the absorption bands.

Ohkoshi *et al.*[10] have previously confronted the birefringence *versus* strain data in the range of draw ratios $1 < \lambda < 6$ with the two most current models for polymer network deformation. They concluded that the affine deformation scheme provides a good fit for draw ratios $\lambda < 2$, while the pseudo-affine scheme is better obeyed for draw ratios $\lambda > 2$, i.e. beyond the onset of the strain-induced crystallization. Voice *et al.*[14] have shown, on the other hand, that the overall orientation function assessed from refractive index measurements in the range of draw ratios $1 < \lambda < 3.5$ is rather approximated by a pseudo-affine model.

In our previous paper[11] concerned with the tensile drawing of PEEK, we paid particular attention to the experimental study of the orientation and stress variations with strain above the glass transition and put forward a molecular mechanism for these variations in relation to the strain-induced crystallization effect. The birefringence, infrared dichroism and shrinkage stress data were analysed in the framework of rubber elasticity at low strains in order to characterize the molecular parameters of the network. It was thus shown that the molecular weight between entanglements is about 3000 and the length of the random link about 1.8 nm. The very low shrinkage stress level at draw ratio below the threshold of the strain-induced crystallization was consistent with a weakly entangled network (i.e. three entanglements per chain on average) that was prone to disentangle under loading. Besides, the birefringence *versus* shrinkage stress plot disclosed an orientation-dominated regime at low strains followed by a deformation-dominated regime after the onset of the strain-induced crystallization due to the incipient physical crosslinking effect of the crystallites.

The present paper reports on modelling the deformation behaviour of amorphous PEEK under tensile drawing, using the orientation–strain and stress–strain data of the first paper of the series. Considering that the sole orientation function determination is in fact unable to account for the mechanical properties of drawn polymers, we have focused on the sophisticated model of Brown and Windle[20,21] which can predict both orientation–strain and stress–strain relationships. In addition, this model affords a quite subtle combination of the two previously quoted approaches since it considers two independent contributions to the strain, namely the extension of the chains and the orientation of the rigid structural units in the chains. Isothermally-crystallized PEEK has been also analysed for the sake of comparison.

EXPERIMENTAL

The material studied was an amorphous film of Stabar K200 from ICI having a thickness of about 50 μm. It was perfectly isotropic as judged from the absence of both measurable birefringence and dimensional shrinkage above the glass transition temperature. Its number average molecular weight estimated from the glass transition and the cold crystallization peak temperatures was $M_n \approx 13\,000$[11]. Semi-crystalline samples having a nominal crystal weight fraction of 29% were prepared by isothermal treatment of amorphous sheets at 170°C for 1 h.

Birefringence, infrared dichroism and shrinkage stress data were taken from the previous paper[11] in the case of amorphous PEEK which was drawn at 160°C. Additional birefringence and infrared dichroism data for semi-crystalline PEEK have been provided according to the procedures described previously, the drawing experiments being performed at 185°C. Shrinkage experiments could not be performed with semi-crystalline PEEK because systematic necking of the samples upon drawing prohibits preparation of sufficiently long test pieces with homogeneous draw ratios.

The crystalline orientation function, f_c, was determined from infrared dichroism measurements on the 965 cm^{-1} vibration band. The amorphous orientation function, f_a, was derived from the equation

$$\Delta n = f_c X_c \Delta n_c^\circ + f_a (1 - X_c) \Delta n_a^\circ \qquad (1)$$

using $\Delta n_a^\circ = 0.38$ and $\Delta n_c^\circ = 0.31$[11]. The crystal weight fraction, X_c, has been assessed from differential scanning calorimetry, assuming a melting enthalpy of perfectly crystalline PEEK of $\Delta H_f = 130\ J\ g^{-1}$ (ref. 22).

THE MODEL

The model of Brown and Windle (B–W)[20,21] is an attempt to combine the affine and pseudo-affine approaches to the deformation of polymers which have been developed to account for chain-extension-dominated and segment-orientation-dominated deformation modes, respectively. Indeed, it deals with the prediction of stress–strain–orientation relationships in rubber networks by taking separately into consideration segment orientation and chain extension effects. It is assumed that the chains are composed of mobile rigid units idealized as prolate ellipsoids of revolution free to undergo independent orientational and extensional motions. However, these structural units are subject to constraints arising from both intramolecular (covalent bonding of the structural units along the chain backbone) and intermolecular (chain entanglements) sources such that, in practice, the two kinds of motions take effect simultaneously and cooperatively.

The model relies on the separation of the overall strain or draw ratio, λ, into an orientational strain, λ_o, and an extensional strain, λ_e, such that

$$\lambda = \lambda_o \times \lambda_e \qquad (2)$$

The calculations of the work involved in the dimensional changes due to both rotation and displacement of the rigid structural units under stress are based on the assumption of Boltzmann distributions of the units in orientation and position with respect to the tensile axis.

Two structural parameters are introduced. The 'form' parameter, m, which is the reciprocal aspect ratio of the rigid structural units is used to account for their orientational behaviour. It is given by

$$1/m = l/a \quad \text{and} \quad m^2 = 1 - e^2 \qquad (3)$$

where l and a are, respectively, the long and the short axis of the ellipsoid of revolution, and e its eccentricity. The 'constraint' parameter, K, represents the intermolecular

and intramolecular interactions limiting the chain extension. It is defined as

$$1/K = N^*/N_o \quad \text{with} \quad K = \lambda_e^{max} \tag{4}$$

where N_o is the total number of structural units, N^* the number of completely constrained structural units, and λ_e^{max} is the maximum value of the extensional strain. It has been shown that K can be related to the density of chain entanglements through the following simple relationship[21]

$$K = \frac{(2/N_s)^{2/3}}{2A_{co}} \tag{5}$$

where N_s is the number per unit volume of chain segments connected with entanglements ($N_s/2$ being the number of entanglements per unit volume) and A_{co} is the mean cross-sectional area per chain at zero strain. At a first approximation, this latter is given by[21]

$$A_{co} = 2S/\alpha \tag{6}$$

α being the packing density and S the cross-sectional area of a chain perpendicular to its axis. The molecular weight of the chain segments between two successive entanglements in the rubbery amorphous phase is then given by

$$M_e = \rho_a N_a / N_s \tag{7}$$

In the present case of PEEK, an estimation of the packing density of the amorphous phase, $\alpha_a = 0.65 \pm 0.01$, can be assessed in consideration of the crystal packing density ($\alpha_c = 0.71 \pm 0.01$) computed from the unit cell volume[23,24] and the van der Waals molecular volume,[25] and the specific gravity ratio of the crystal and the amorphous phase $\rho_c/\rho_c = 1.09$ (ref. 23). Besides, the cross-sectional area of a chain perpendicular to its axis can be approximated by

$$S = V/L \quad \text{with} \quad V = M/\rho_a N_a \tag{8}$$

where V, L and M are the volume, the extended length and the molar weight of the repeat unit (*Figure 1*), respectively, and N_a is the Avogadro number. For PEEK, $L = 1.50 \pm 0.01$ nm[23,24], $M = 288$ g mol^{-1} and $\rho_a \approx 1.26$[23].

An important point of the model is that the variation with stress of second moment of the orientation distribution function, $\langle P_2 \rangle$, otherwise Hermann's orientation function, f, depends only on the aspect ratio of the rigid structural units. It is worth noting that this is analogous to the stress optical coefficient dependence on the statistical segment length in the affine deformation theory[11]. On the other hand, the stress variation with the overall strain depends on both the aspect ratio and the constraint parameter.

The method for deriving the maximum orientational strain together with the aspect ratio of the structural units is briefly described in the Appendix, the whole procedure being given in the second paper by Brown and Windle[21].

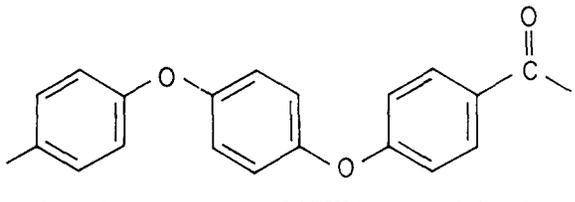

Figure 1 Molecular repeat unit of PEEK in its extended conformation

The $\langle P_2 \rangle$ *versus* λ and σ *versus* λ experimental curves have been compared with the theoretical predictions involving a unique value of the aspect ratio obtained from the procedure described. It has been emphasized by Brown and Windle[21] that 'the model, as it stands, makes no allowance for the pulling out of entanglements' so that the K parameter should also be a constant. Nevertheless, a series of theoretical curves with various values of K have been drawn for comparison with the experimental data, the reason for this being that the entangled chain network can be assumed transient *a priori* because it does not involve chemical crosslinking. It is our belief that a departure from the model may be interpreted as a change in the entanglement density of the physical network upon straining as far as the model works fairly well under conditions which prevent disentanglement.

RESULTS AND DISCUSSION

Amorphous PEEK

The determination of the aspect ratio of the rigid structural units from the initial slope of the $\langle P_2 \rangle$ *versus* λ experimental curve according to the method described in the Appendix leads to a value $1/m = 3.1$. This indicates that the structural units consist approximately of a single monomer unit which is indeed one phenyl wide and three phenyl long (see *Figure 1*). A quite favourable comparison can be made with the size of the random link previously determined from an independent measurement of the stress-optical coefficient in the strain range beyond the strain-induced crystallization threshold in the framework of the affine theory of rubber elasticity, and owing to the knowledge of the optical anisotropy of the monomer unit[11]. As a matter of fact, these two structural parameters are necessarily connected since they both relate to the stiffness of the chains.

The overall birefringence variation reported in our previous study could be correctly predicted neither by the affine deformation model nor by the pseudo-affine one over the whole range of draw ratio. The same comment is applicable to the variation with draw ratio of the amorphous orientation function, f_a shown in *Figure 2*.

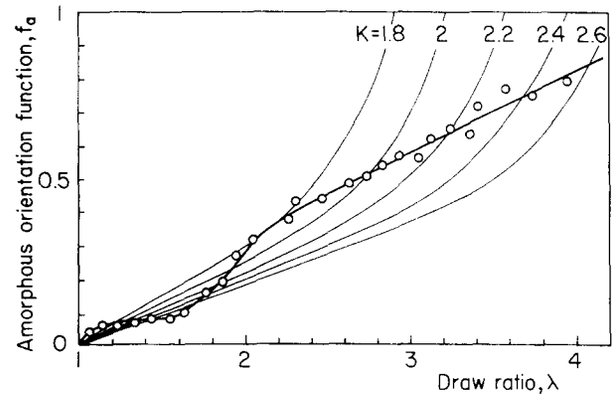

Figure 2 Amorphous orientation function data *versus* draw ratio for initially amorphous PEEK compared with the predictions from the Brown and Windle model using various values of K and assuming $1/m = 3.1$

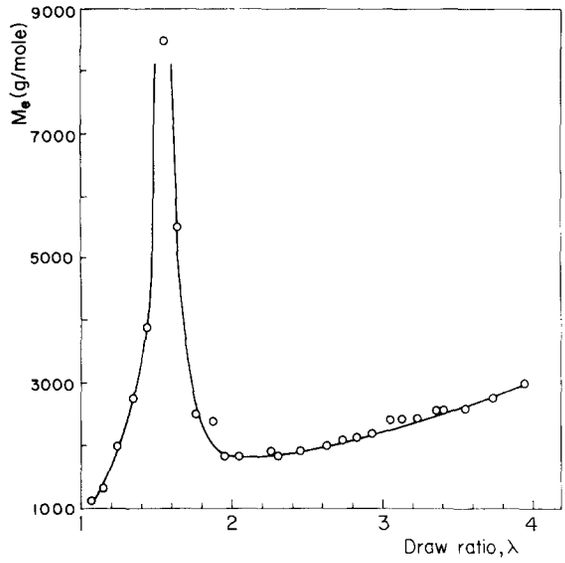

Figure 3 Variation with draw ratio of the molecular weight between entanglements, M_e, assessed from the Brown and Windle model using the orientation function data of *Figure 2*

The theoretical predictions from the B–W model are drawn for various values of the K parameter, assuming $1/m = 3.1$ as determined above. At small strains, the smoothed curve from the experimental data cuts the theoretical curves corresponding to increasing values of K. This suggests slippage and disentanglement of the chains in a very slightly intertwined rubber network. But at the early stage of the strain-induced crystallization[11], i.e. $1.6 < \lambda < 1.8$, the smoothed curve from the experimental data displays a higher slope than the theoretical curves, then roughly follows the curves of nearly constant $K \approx 1.8$–2.0 in the strain range $1.9 < \lambda < 2.8$. The build-up of crystallites gradually brings about new physical crosslinks due to the anchoring of the amorphous chain portions onto the surface of the crystallites which prevent further disentanglement of the chains. For $\lambda > 2.8$ up to rupture, the decrease of the f_a *versus* λ slope is associated with a decrease of the K parameter which is relevant to a reduction of the effective density of entanglements including the physical crosslinks of the crystallites. Indeed, at the relatively high temperature of the experiments, i.e. 160°C, the ductility of the crystallites may allow the pulling out of chains under high stress, notably the numerous chain ends.

The molecular weight between entanglements computed according to equation (7) from the experimental data of the amorphous orientation function of *Figure 2* is plotted in *Figure 3* as a function of the draw ratio. The extrapolated value $M_e \approx 1000$ at $\lambda = 1$ is significantly lower than the previous determination from the classical theory of rubber elasticity at low strains[11], namely $M_e \approx 3000$*, which is close to that reported for bisphenol A polycarbonate and poly(2,6-dimethyl-1,4-phenylene oxide), two structural homologues of PEEK[26]. However, it is noteworthy that copolymers of bisphenol A carbonate with terephthalate or isophthalate esters have significantly lower M_e values[27]. So, taking into account the numerous approximations involved in the calculations, the two determinations can be considered as the same order of magnitude.

Notwithstanding this disagreement, the increase of M_e by about 10 times in the range $1 < \lambda < 1.6$ (*Figure 3*) suggests that most of the short chains have been completely disentangled due to chain slippage. This statement is well supported by the maximum value of $M_e \approx 9000$ which is only slightly lower than the number average molecular weight, indicating that there are few remaining entanglements at $\lambda \approx 1.6$. The subsequent drop to a roughly constant value $M_e \approx 2000 \pm 200$ in the intermediate draw ratio range, $1.9 < \lambda < 2.8$, where the strain-induced crystallization takes place gives a quantitative indication of the physical crosslinking effect of the crystallites. All this is perfectly consistent with the qualitative conclusions of our previous study.

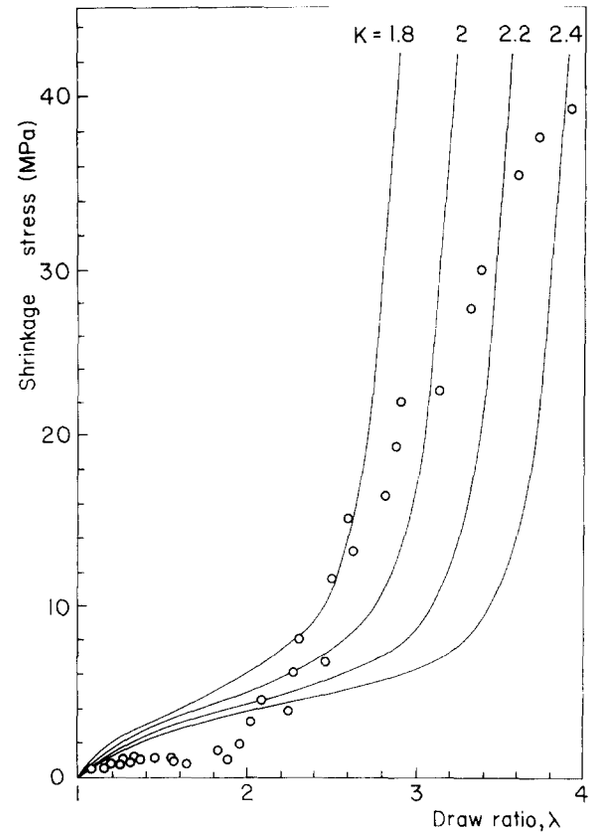

Figure 4 True stress data *versus* draw ratio for initially amorphous PEEK compared with the predictions from the model of Brown and Windle using various values of K and assuming $1/m = 3.1$

The variation of the true stress as a function of draw ratio is shown in *Figure 4*. Predictions from the B–W model are drawn for various values of the K parameter, assuming $1/m = 3.1$. At low strains, the experimental data fall well below the curves predicted for the same values of K that fit the orientation function data of *Figure 2*. This suggests that the actual strain experienced by the chains is far below the draw ratio measured macroscopically. In other words, the strain due to chain slippage is large compared with the strain resulting from chain extension, both strains being gathered in the measured overall strain or draw ratio together with the orientational strain. However, as soon as the strain-induced crystallization takes place, the stress displays a drastic increase which follows a theoretical curve of a

* The value of the molar weight between entanglements reported in the former paper[11] is a misprint. It should read $M_e \approx 3000$ instead of 2000

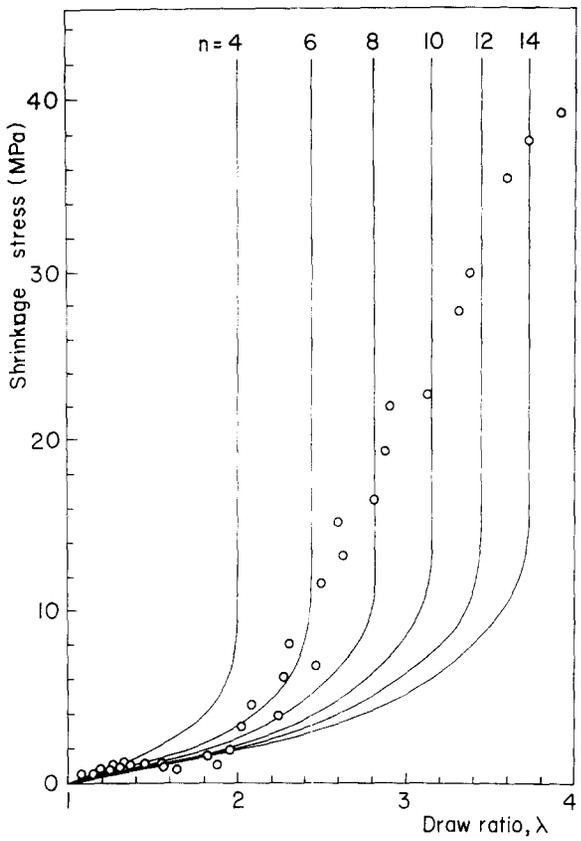

Figure 5 True stress data of *Figure 3* compared with the predictions from the affine non-gaussian deformation model using various values of N

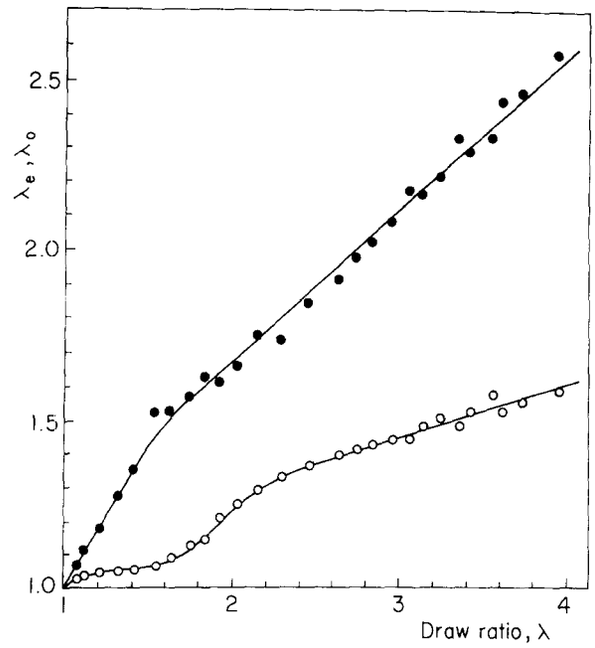

Figure 6 Variation with the overall strain, λ, of the orientational strain, λ_o (○) and the extensional strain, λ_e (●), for initially amorphous PEEK

fairly constant value of $K \approx 1.8$–2.0 which is remarkably consistent with the one that fits the amorphous orientation function in the same strain range (*Figure 2*). For $\lambda > 2.8$, the departure of the experimental data from the theoretical curves predicting a steady high slope confirm the gradual decay of the entanglement effect of the crystallites before rupture.

It is worth noting that the true stress data of *Figure 4* displays a much more important departure from the predicted curves at low strains than the orientation function data of *Figure 2*. This means that the disentanglement of the chains that occurs at the beginning of straining is much more detrimental for chain extension than for chain orientation.

For the sake of comparison, the data of *Figure 4* are redrawn in *Figure 5* together with theoretical curves predicted from the affine non-gaussian deformation model according to the relationship[3]

$$\sigma = \frac{N_s kT}{3} n^{1/2} \left\{ L^{-1}\left(\frac{\lambda}{n^{1/2}}\right) - \lambda^{-3/2} L^{-1}\left(\frac{1}{\lambda^{1/2} n^{1/2}}\right) \right\} \tag{9}$$

where N_s is the number per unit volume of chain segments connected with entanglements as already defined in equation (5), n is the length of these chain segments expressed as the number of random links between entanglements and L^{-1} is the inverse Langevin function. Although somewhat different from the B–W predictions, the latter ones suggest the same trend, the experimental data in the low strain range being indeed significantly lower than the theoretical curve of nearly constant n value that fits the intermediate strain range after the onset of the strain-induced crystallization. In this strain range, the molecular weight between entanglements, $M_e \approx 2000 \pm 300$ calculated from $n = 7 \pm 1$ (*Figure 5*) and taking into account that the random link is composed of a single monomer unit[11], is perfectly consistent with the value derived from K of the B–W model, from both orientation and stress data.

The variations with the overall strain or draw ratio of the orientational and extensional strains, λ_o and λ_e respectively, are shown in *Figure 6* (see Appendix, equations (A2) and (A3)). The first observation is that λ_e is always greater than λ_o. This result is quite surprising and seems to contradict the conclusion from our previous study[11] that the early stage of the deformation is orientation dominated. In fact, the orientational strain which mainly depends on the chain stiffness (see Appendix, the unique relationship (equation (A6)) between the aspect ratio and λ_o^{max}) is much more limited than the extensional strain. This is clearly depicted in *Figure 7* which shows schematically the maximum strain that a polymer coil can reach through either orientation of the structural units alone or extension of the chains without orientation of the structural units. In the case of PEEK, the maximum value of the orientational strain is $\lambda_o^{max} = 1.66$ according to the method described in the Appendix, using the aspect ratio $1/m = 3.1$. The second observation is that, from the onset of the strain-induced crystallization at $\lambda \approx 1.8$, the slope of the variation with the overall strain of λ_o undergoes a sudden increase while that of λ_e displays a striking decrease. The reason is that the growth of crystallites which work as crosslink points in the physical network reduces the apparent chain extension by preventing the chain slippage contribution to λ_e and *per contra* improves the orientation trend of the structural units. In fact, although the two contributions have been treated independently in the model, they obviously take place cooperatively. It is worth noting that the general trend of the λ_o variation (*Figure 6*)

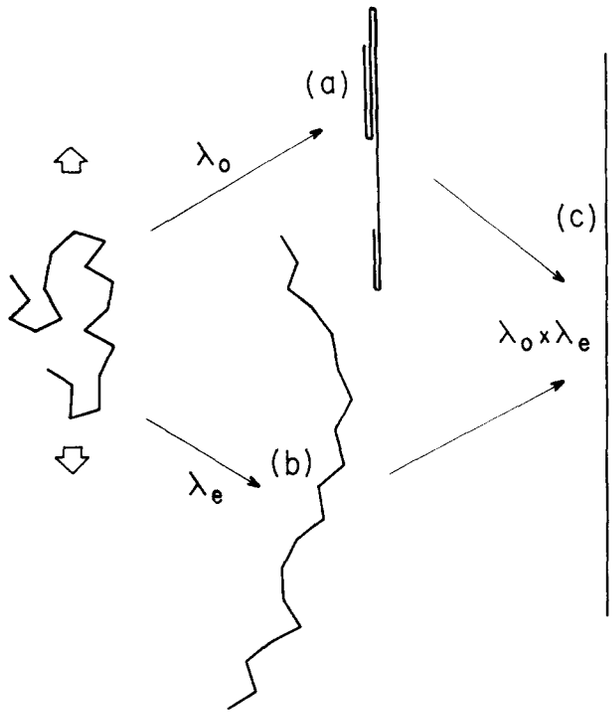

Figure 7 Molecular sketch showing the separate development of (a) the orientational strain and (b) the extensional strain of a single coil in a polymer network under uniaxial tensile deformation, and (c) the resulting overall strain[20]

follows remarkably the f_a variation shown in *Figure 2*. The limiting value at rupture $\lambda_o = 1.6$ approaches logically the theoretical value $\lambda_o^{max} = 1.66$ assessed previously from the model for a structural unit having an aspect ratio $1/m = 3.1$. But this result has relevance only through the unusually high value of the limiting amorphous orientation function $f_a^{max} \approx 0.8$ and $\lambda \approx 4$ (see *Figure 2*), since λ_o^{max} assumes a perfect orientation of the chain segments. In this connection, the negative thermal expansivity coefficient reported by Choy *et al.*[9] and Lee *et al.*[13] for PEEK sheets and rods of draw ratios $\lambda \approx 4$–5 is also relevant to a high degree of orientation in both the amorphous phase and the crystal.

The above discussion strongly suggests that crystallization is orientation-induced rather than strain-induced. In this connection, it has been shown clearly in the case of poly(ethylene terephthalate) that the main factor which controls the crystallization kinetics under straining at temperatures well below the temperature range of thermal crystallization is the amorphous orientation function[28,29]. Besides, it is worth mentioning that, dealing with the crystallization under strain, amorphous PEEK is more similar to poly(ethylene terephthalate) and poly(ethylene naphthalate) than to its structural relatives bisphenol A polycarbonate and poly(2,6-dimethyl-1,4-phenylene oxide) despite the fact that it is closer to the last two polymers as concerns the glass transition temperature. Although potentially crystallizable, these two polymers have stronger steric hindrance than PEEK due to substitution groups that considerably slow down the crystallization kinetics.

The disentanglement of the chains is likely to be due to the low number average molecular weight of the chains which allows little intertwining of the chains and therefore makes chain slippage an easy process. In this

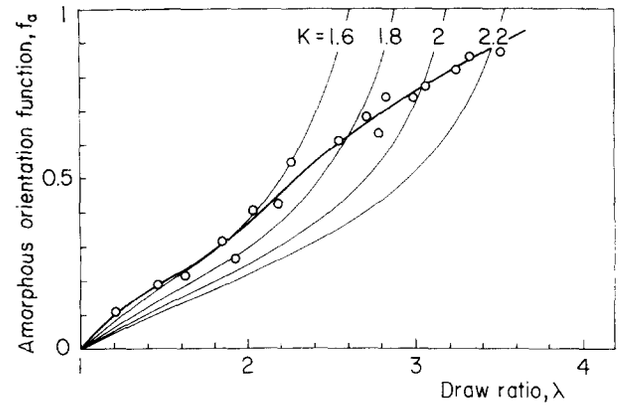

Figure 8 Amorphous orientation function data *versus* draw ratio for isothermally-crystallized PEEK compared with the predictions from the model of Brown and Windle using various values of K and assuming $1/m = 3.1$

connection, it has been shown that low molecular weight amorphous poly(ethylene terephthalate)[30] as well as poly(ethylene naphthalate)[31,32] are strongly prone to chain disentanglement when drawn a few degrees above the glass transition temperature. However, the process hardly occurs for poly(ethylene terephthalate) of molecular weight higher than 25000 which contains more than 10 entanglements per chain[30].

Isothermally-crystallized PEEK

The change of temperature for the drawing of semi-crystalline PEEK compared with amorphous PEEK, i.e. 185°C instead of 160°C, is of little importance in the determination of the key parameters of the deformation from the procedure described in the Appendix, namely m, K and λ_o^{max}.

The aspect ratio estimated from the initial slope of the $\langle P_2 \rangle$ *versus* λ experimental curve, $1/m = 3.1$, is in very good agreement with that found for the amorphous PEEK. This result is quite logical since the aspect ratio of the rigid structural unit must be an intrinsic property of the chain which only depends on its chemical nature.

The variation with draw ratio of the amorphous orientation function is shown in *Figure 8*. Predictions from the B–W model are drawn for various values of the K parameter, assuming $1/m = 3.1$ as determined above. In the strain range $1 < \lambda < 2.5$, the smoothed experimental f_a *versus* λ curve falls fairly well between the theoretical curves predicted for $K = 1.6$–1.8, but a significant divergence appears for $\lambda > 2.5$. Compared with the previous case of amorphous PEEK, this result is a clear indication of the efficiency of the pre-existing crystallites for preventing chain slippage at low moderator stress. The molecular weight between entanglements computed for every experimental data point of *Figure 8* is plotted in *Figure 9* as a function of the draw ratio. The average M_e value hardly changes in the strain range $1 < \lambda < 2.5$ indicating that little change occurs in the entanglement density including the crystallite physical crosslinks, in spite of the large plastic deformation of the crystallites. Comparison with amorphous PEEK (*Figure 3*) shows that the entanglement density is very close for both materials in the strain range $\lambda > 1.9$. This strongly suggests that physical crosslinking is more efficient than chain entanglements and that the loss of

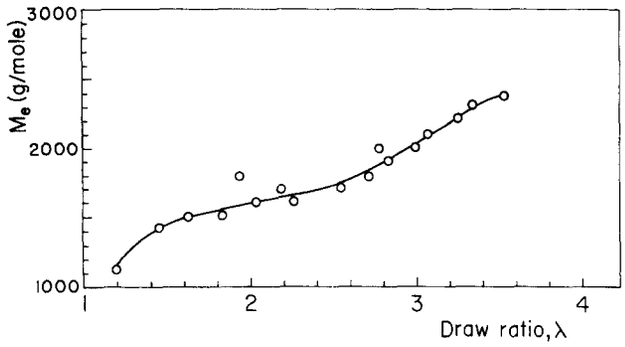

Figure 9 Variation with draw ratio of the molecular weight between entanglements, M_e, for isothermally-crystallized PEEK

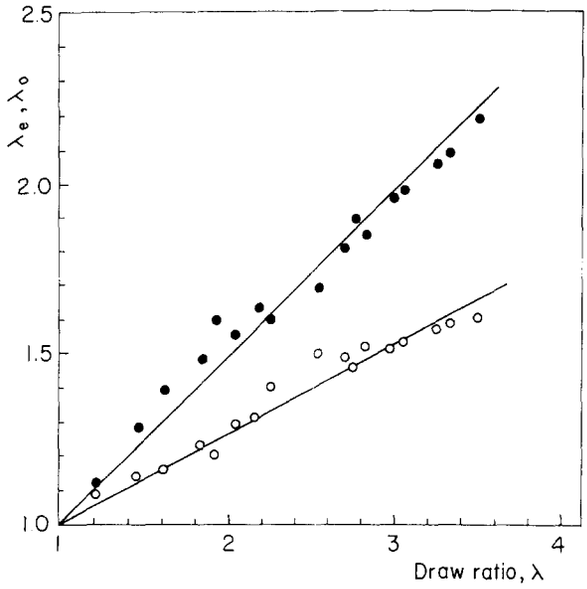

Figure 10 Variation with the overall strain, λ, of the orientational strain, λ_0 (○), and the extensional strain, λ_e (●), for isothermally-crystallized PEEK

entanglements that occurred in the initial stage of the deformation of amorphous PEEK has no significant incidence on the subsequent deformation behaviour.

The variations with the overall strain, λ, of the orientational and extensional strains, λ_0 and λ_e respectively, are shown in *Figure 10*. Both contributions vary almost linearly with the overall strain indicating that plastic deformation involves a combination of continuous mechanisms of chain unfolding and segment orientation over the whole strain range due to the physical crosslinking effect of the crystallites.

CONCLUSION

The Brown and Windle model is not suitable for predicting the stress–strain–orientation behaviour of PEEK under tensile drawing. However, its use is very helpful for understanding the mechanisms of chain unfolding along with strain. The main conclusions are the following.

(1) The rigid structural units are shown to be of the size of the statistical segment, i.e. a single repeat unit. Their strong geometrical anisotropy (i.e. aspect ratio close to 3) may be responsible for the strong orientational behaviour at the beginning of drawing.

(2) The evolution of the molecular weight between entanglements of amorphous PEEK computed from the model clearly shows a disentanglement of the chains prior to the strain-induced crystallization followed by an increase of the entanglement density due to the gradual growth of crystallites.

(3) In parallel, the model suggests that no significant change in the entanglement density occurs for crystalline PEEK, up to the strain range preceding rupture, due to the initial pressure of crystallites.

REFERENCES

1 Ward, I. M. (Ed.) 'Developments in Oriented Polymers', Applied Science Publishers, London, 1982
2 Zachariades, A. E. and Porter, R. S. 'The Strength and Stiffness of Polymers' (Eds A. E. Zachariades and R. S. Porter), M. Dekker Inc., New York, 1983
3 Treloar, L. R. G. 'The Physics of Rubber Elasticity', 2nd edn, Clarendon Press, Oxford, 1958
4 Ward, I. M. *Adv. Polym. Sci.* 1985, **66**, 81
5 Rietsch, F. *Eur. Polym. J.* 1985, **21**, 793
6 Arruda, E. M. and Boyce, M. C. *J. Mech. Phys. Solids* 1993, **41**, 389
7 Wu, M. C. and van der Giessen, E. *J. Mech. Phys. Solids* 1993, **41**, 427
8 Ward, I. M. *J. Polym. Sci. Polym. Symp.* 1977, **58**, 1
9 Choy, C. L., Leung, W. P. and Nakafuku, C. *J. Polym. Sci. Polym. Phys. Ed.* 1990, **28**, 1965
10 Ohkoshi, Y., Ohshima, H., Matsuhisa, T., Toriumi, K. and Konda, A. *Sen-i-Gakkaishi* 1989, **45**, 509
11 Bassigny, V., Séguéla, R., Rietsch, F. and Jasse, B. *Polymer* 1993, **34**, 4032
12 Rueda, D. R., Ania, F., Richardson, A., Ward, I. M. and Balta-Calleja, F. J. *Polym. Commun.* 1983, **24**, 258
13 Lee, Y., Lefebvre, J.-M. and Porter, R. S. *J. Polym. Sci. Polym. Phys. Ed.* 1988, **26**, 795
14 Voice, A. M., Bower, D. I. and Ward, I. M. *Polymer* 1993, **34**, 1154
15 Chalmers, J. M., Gaskin, W. F. and Mackenzie, M. W. *Polym. Bull* 1984, **11**, 433
16 Nguyen, H. X. and Ishida, H. *Polymer* 1986, **27**, 1400
17 Nguyen, H. X. and Ishida, H. *J. Polym. Sci. Polym. Phys. Ed.* 1986, **24**, 1079
18 Jonas, A., Legras, R. and Issi, J.-P. *Polymer* 1991, **32**, 3364
19 Voice, A. M., Bower, D. I. and Ward, I. M. *Polymer* 1993, **34**, 1164
20 Brown, D. J. and Windle, A. H. *J. Mater. Sci.* 1984, **19**, 1997
21 Brown, D. J. and Windle, A. H. *J. Mater. Sci.* 1984, **19**, 2013
22 Blundell, D. J. and Osborn, B. N. *Polymer* 1983, **24**, 953
23 Hay, J. N., Kemmish, D. J., Langford, J. I. and Rae, A. I. M. *Polymer Commun* 1984, **25**, 175
24 Fratini, A. V., Cross, E. M., Whitaker, R. B. and Adams, W. W. *Polymer* 1986, **27**, 861
25 Wunderlich, B. 'Macromolecular Physics: Crystal Structure, Morphology, Defects; Vol. 1', Academic Press, New York, 1973
26 Donald, A. M. and Kramer, E. J. *J. Polym. Sci. Polym. Phys. Ed.* 1982, **20**, 899
27 Prevorsek, D. C. and de Bona, B. T. *J. Macromol. Sci. Phys.* 1986, **B25**, 515
28 le Bourvellec, G., Jarry, J. P. and Monnerie, L. *Polymer* 1986, **27**, 856
29 le Bourvellec, G., Monnerie, L. and Jarry, J. P. *Polymer* 1987, **28**, 1712
30 Engelaere, J.-C., Cavrot, J.-P. and Rietsch, F. *Polymer* 1982, **23**, 766
31 Ghanem, A. M. and Porter, R. S. *J. Polym. Sci. Polym. Phys. Ed.* 1989, **27**, 2587
32 Ito, M., Honda, K. and Kanamoto, T. *J. Appl. Polym. Sci.* 1992, **46**, 1013

APPENDIX

The Brown and Windle approach of the uniaxial tensile deformation of rubber networks is based on the description of the orientation and position with respect to the tensile axis of rigid structural units in terms of Boltzman distributions for the calculations of the work done by the applied stress for both rotating and displacing these units[21]. For doing this, the following dimensionless variable has been introduced

$$q = \sigma v/kT \qquad \text{(A1)}$$

where σ is the true stress, v is the volume of the structural unit, k is the Boltzman constant and T is the absolute temperature.

A set of plots of the initial slope of the λ *versus* q relationship, i.e. $(d\lambda/dq)_o$, as a function of the initial slope of the $\langle P_2\rangle$ *versus* q relationship i.e. $(d\langle P_2\rangle/dq)_o$, both predicted from the model, are drawn for various values of the constraint parameter K. This is shown in *Figure 11*. These plots have been computed numerically because they cannot be represented by analytical expressions[21]. The relevant equations involved in the calculations of the λ *versus* q function are the following

$$\lambda_o = \frac{2m}{1 + (m^2/e)Ln[(1+e)/m]} \times \frac{I_3}{I_2} \qquad \text{(A2)}$$

and

$$\lambda_e = 1/[(1/K) + (1 - 1/K)\exp(-q)] \qquad \text{(A3)}$$

where $I_n = \int \sec^{q+n}\psi \, d\psi$ between the limits $\psi = \arccos m$ and $\psi = \arccos 1 = 0$, and reminding that $\lambda = \lambda_o \times \lambda_e$.

The calculations of the $\langle P_2\rangle$ *versus* q function are based on the relationships

$$\langle P_2(\cos\theta)\rangle = 1/2(3\langle\cos^2\theta\rangle - 1) \qquad \text{(A4)}$$

with

$$\langle\cos^2\theta\rangle = \frac{m^2}{e^2} \times \frac{I_4 - I_2}{I_2} \qquad \text{(A5)}$$

Every curve of *Figure A1* is obtained by varying m at constant K.

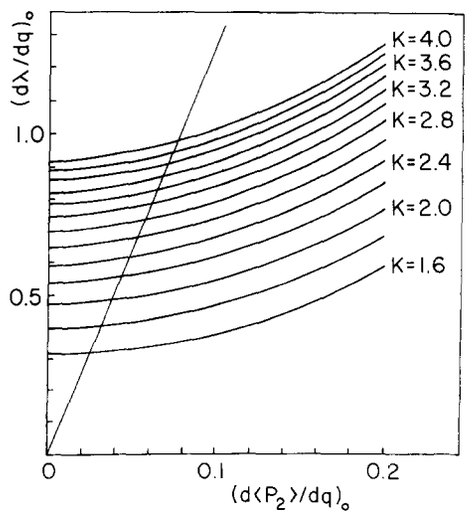

Figure A1 Predicted plots of the reciprocal initial slope $(d\lambda/dq)_o$, of the $q = f(\lambda)$ function *versus* the initial slope $(d\langle P_2\rangle/dq)_o$, of the $\langle P_2\rangle = f(q)$ function, for various values of the constraint parameter K. The intersecting straight line has a slope equal to the experimental value $(d\lambda/d\langle P_2\rangle)_o = 0.078$ (see the text for details)

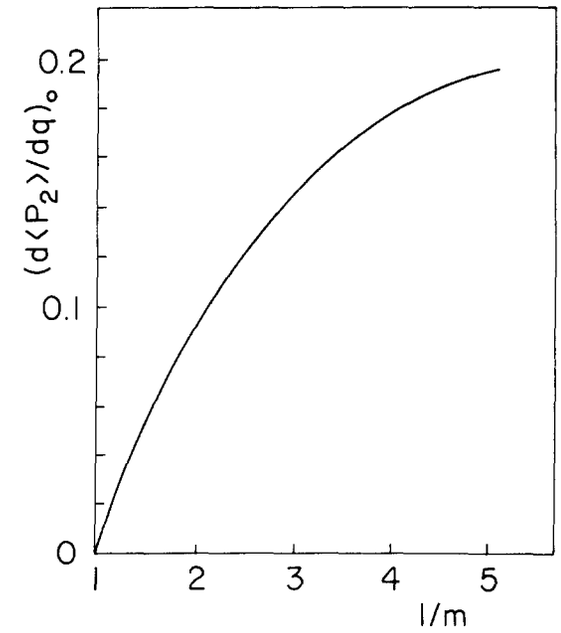

Figure A2 Variation curve of $(d\langle P_2\rangle/dq)_o$ as a function of the aspect ratio $1/m$

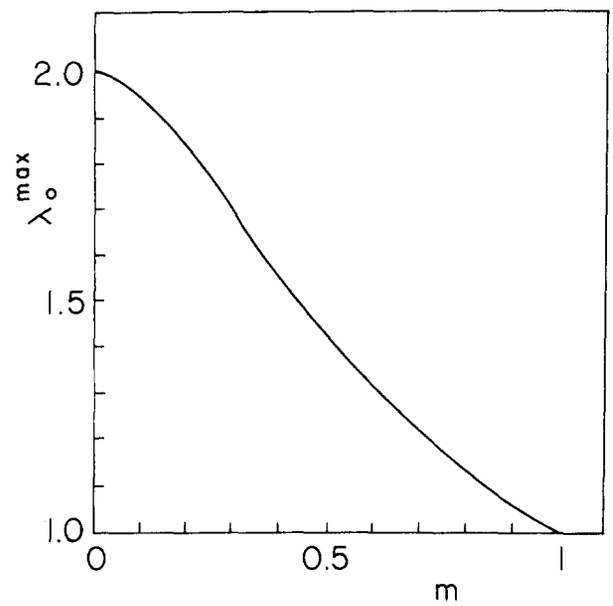

Figure A3 Variation curve of the maximum orientational strain, λ_o^{max}, as a function of the reciprocal aspect ratio, m

A straight line of gradient equal to the experimental value of the reciprocal initial slope of the $\langle P_2\rangle$ *versus* λ curve, i.e. $(d\lambda/d\langle P_2\rangle)_o$, is then drawn through the previous set of curves. The intersection with every curve corresponding to a particular value of K gives an abscissa $(d\langle P_2\rangle/dq)_o$ from which a value of the aspect ratio, $1/m$, is obtained graphically from *Figure A2*. This latter figure relies on the sole dependence on m of the $\langle P_2\rangle$ *versus* q function given above.

Using the aspect ratio value, the maximum orientational strain, λ_o^{max}, is derived from *Figure A3* according to the relationship

$$\lambda_o^{max} = 2 \Big/ \left[1 + \frac{m^2}{e} Ln\left(\frac{1+3}{m}\right)\right] \qquad \text{(A6)}$$

Finally, λ^{max} assessed from the product $\lambda_o^{max} \times K$ is compared with the experimental maximum strain. By successive adjustments of K, the whole procedure is performed until agreement between the predicted and the experimental values of λ^{max} for the final determination of $1/m$ and λ_o^{max}.

Finally, plotting the stress–strain and orientation–strain curves has been made by using the specific data for the present study of PEEK, namely the temperature of drawing, i.e. 160°C, and the volume of the structural unit which is close to that of a monomer unit, i.e. $V \approx 0.60\,nm^3$ (see equation (8)).